Carbon Nanotubes

Self-Assembly of Large-Scale Micropatterns on Aligned Carbon Nanotube Films**

Huan Liu, Shuhong Li, Jin Zhai, Huanjun Li, Quanshui Zheng, Lei Jiang, and Daoben Zhu*

The fabrication of well-defined structures with nanoscale materials is a key technology,[1] and self-assembly is an efficient and often preferred process to build micro- and nanoparticles into ordered macroscopic structures.[2] As carbon nanotubes are attractive materials for nanotechnology because of their interesting physicochemical properties and molecular symmetries,[3–6] it is necessary to control the architecture of carbon nanotubes on the substrates. Most patterned carbon nanotubes are formed on prepatterned substrates or prepatterned catalysts during the fabrication process.[7–9] Herein we report the first use of a long-range force (capillary force) in the self-assembly of three-dimensional (3D) micropatterns on aligned carbon nanotube films through a water-spreading method after the growth of the carbon nanotube. It is considered that low-density regions or vacancies of carbon nanotube films play an important role in the formation of the pattern. Therefore different kinds of highly ordered micropatterned structures have been built in a controlled fashion by introducing vacancies artificially.

Hydrophobic aligned carbon nanotube films were grown on quartz substrates by pyrolysis of iron(II) phthalocyanine (FePc) by methods described in the literature.[10–12]

Interestingly, when a water droplet was placed on the fresh carbon nanotube film, the color of the water region changed from black to grey. Water permeates slowly into the film, accompanied by a change in the height and shape of the droplet, but its contact area with the film is almost unchanged (See Supporting Information Figure S1). Detailed scanning electron microscopic (SEM) observations show that the structures in the grey color region are micropatterns composed of honeycomb-like polygons with sizes ranging from 30 to 60 μm (Figure 1 a). An oblique view shows that these

[*] Dr. H. Liu,[+] Dr. S. Li,[+] Dr. J. Zhai, Dr. H. Li, L. Jiang, D. Zhu
Center of Molecular Sciences, Institute of Chemistry,
Chinese Academy of Sciences
Beijing 100080 (P. R. China)
Fax: (+86) 10-8262-7566
E-mail: jianglei@infoc3.icas.ac.cn
Prof. Q. Zheng
Tsinghua University
Beijing 100084 (P. R. China)

[+] PhD students of the Graduate School of the Chinese Academy of Sciences. They contributed equally to this work.

[**] The authors thank the State Key Project Fundamental Research (G1999064504) and the Special Research Foundation of the National Nature Science Foundation of China (29992530) for continuing financial support. The Chinese Academy of Sciences is gratefully acknowledged.

Supporting information for this article is available on the WWW under http://www.angewandte.org or from the author.

  DOI: 10.1002/ange.200351988

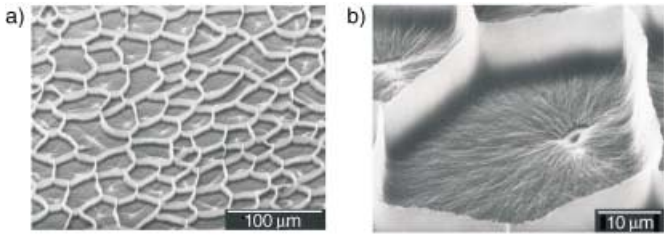

Figure 1. a) The SEM image of patterned carbon nanotubes induced by water spreading. These patterns are mostly honeycomb-like structures with the sizes ranged from 30 to 60 μm. b) Enlarged oblique view of an individual honeycomb structure with the honeycomb "wall" vertical to the substrate.

honeycomb-like patterns have 3D structures in which the "walls" are vertical to the substrate. Figure 1b is a high-resolution SEM image of an individual polygon. All carbon nanotubes inside this polygon are bent radially toward the "walls" from the center. In particular, all carbon nanotubes originally on the substrate of the "cave" region were flattened, bundled, and eventually formed the cave (See Supporting Information Figure S2). The height and thickness of the "walls" are 6–10 μm and ca. 0.5 μm, respectively, in this image.

All these phenomena can be explained as the self-assembly of carbon nanotubes as a result of the capillary action of water. A variety of strategies for self-assembly have been proposed and employed to fabricate two- and three-dimensional structures,[13–18] and the driving forces are usually van der Waals forces,[19] hydrogen bonding,[20] and Coulombic forces.[21,22] However, these short-range forces can only act on a molecular level, whereas longer-range forces, such as surface tension, capillary force, convection, etc., can be used for constructing microstructures with nanostructured materials. Although carbon is hydrophobic, it is known that flat graphite surfaces are hydrophilic, with a water contact angle ϕ_g of $\approx 86°$.[22] Transmission electron microscopy images (See Supporting Information Figure S3) of carbon nanotubes dispersed from the film show their bamboolike structure, with diameters ranging from 40 to 60 nm. We have not found measurement water contact angle values of carbon nanotubes. However, it is believed that the water contact angle of perfect carbon nanotubes of large diameters (40–60 nm) would be almost the same as that of the graphite plane. The bamboo structures should lead to better hydrophilicity than that of perfect nanotubes, as generally observed for that of rough surfaces. This means that the water contact angles ϕ_{nt} of the bamboolike carbon nanotubes are generally smaller than 86°. The SEM image of the film surface (See Supporting Information Figure S4) shows that thinner tubes extend from thicker aligned tubes and grovel on the film surface. These hydrophilic flattened tubes guide the water droplet along the corresponding aligned carbon nanotubes into the film.

Once the water is guided into the spaces between the aligned tubes, the resulting capillary action forces the water down to the quartz substrate. The water then spreads over the substrate because the quartz is hydrophilic. All interspaces among aligned tubes over the water-spread region become to be soaked due to the capillary force. The capillary force supplied by a single nanotube of radius r can be estimated to be $2\pi r\gamma_w \cos\phi_{nt}$ through the water surface tension or surface energy[23] $\gamma_w = 72.8\ mN\,m^{-1}$ and the water contact angle ϕ_{nt}. The capillary force thus generates a hydrostatic dilation stress p to the water. To have an estimate of p, we modeled an aligned carbon nanotube cluster by a hexagonal distribution of their cross-section (Figure 2a,b), with diameter $2r$ and distance $2R$ of tubes, which gives rise to Equation (1), in which $c = (rR^{-1})^2$ is the density of carbon nanotubes.

$$p = \frac{2r\gamma_w \cos\phi_{nt}}{R^2 - r^2} = p_{0.5}\frac{c}{1-c},\ p_{0.5}\frac{2\gamma_w \cos\phi_{nt}}{r}, \qquad (1)$$

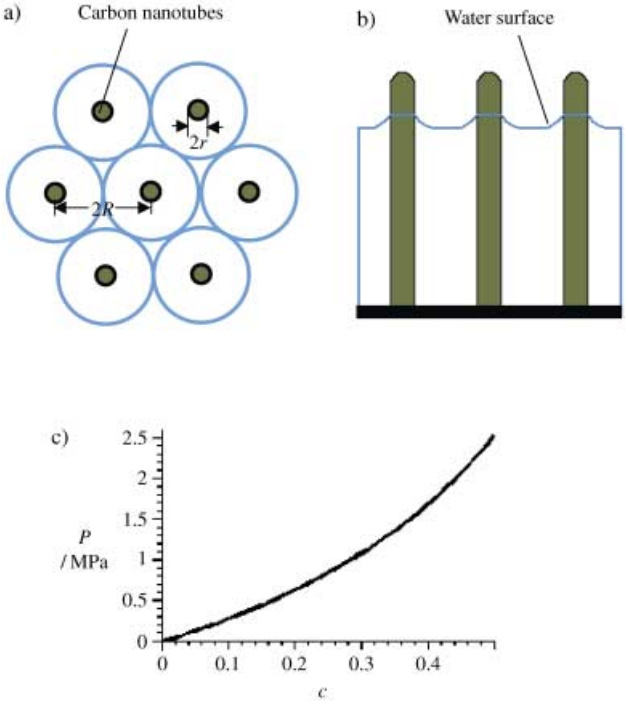

Figure 2. a) Top view and b) side view of the model of the aligned carbon nanotube cluster with tubes of diameter $2r$ at a distance $2R$. The blue lines represent the water surface, the dark green dots and pillars are the carbon nanotubes. c) The relationship between hydrostatic dilation stress p and the volume fraction of nanotubes.

Using the values $\gamma_w = 72.8\ mN\,m^{-1}$, $r = 40$ nm, $\phi_{nt} < \phi_g = 86°$ yields $p > (0.25c)(1-c)^{-1}$ in MPa. The relationship between the dilation stress p and the volume fraction of nanotubes c is shown in Figure 2c, indicating the nonlinear increase in p as the carbon nanotube density increases. This hydrostatic dilation stress alone causes the nanotubes to flatten.

SEM images of the grown carbon nanotube films show that the carbon nanotube densities are not homogeneous. There are both low-density and high-density regions in all carbon nanotube films. With the above estimate of hydrostatic dilation stress p, the nanotubes along the boundary between a lower-density $-c_l$ and higher-density $-c_h$ regions are subjected to a load q per unit tube length toward the higher-density region (Equation (2)).

$$q = p_{0.5}\, r\left(\frac{\sqrt{c_h}}{1-c_h} - \frac{\sqrt{c_l}}{1-c_l}\right) \qquad (2)$$

From Equation (2) it can be concluded that aligned nanotubes may be bent, flattened, or even burst through from lower- toward higher-density regions. For example, with the observed typical values $R_h r^{-1} = 2$ and $R_l r^{-1} = 3$, we have $q = 3.7 \times 10^{-3}$ N m^{-1}. The bundling force and bending moment experienced by a single nanotube of length $L = 19$ μm near the substrate are $qL = 70.3$ nN and $(qL^2)/2 = 6.7 \times 10^{-4}$ nN m, respectively. If the axial Young modulus of the carbon nanotubes is assumed to be 1 TPa, then the maximum bending strain is 11 %, that is, much larger than the critical rippling strain of ≈ 0.6 %.[24,25] It means that the estimated load q experienced by a single carbon nanotube can even force a dozen carbon nanotubes to be severely bent. During the above bending and bundling procedures, $-c_l$ decreases and $-c_h$ increases further. This leads to a stronger and stronger q, until micropatterns are formed in which nanotubes are very closely aligned so that the van der Waals repulsive forces between the nanotubes become effective and balance q. That is, the hydrostatic dilation stress at higher densities is larger than that at lower densities, so this difference leads to the flattening of the nanotubes, while the "wall" is formed when the collapsing nanotubes from opposite directions meet between two regions of lower density. The lower-density region is the center of the micropatterns.

Therefore, it is possible to control the patterns artificially, for example, to etch the regular vacancies by pulse laser. The vacancy etched by laser is 2–3 μm in diameter and various patterns with different vacancy distances were prepared when a water droplet was placed on the surface. Figure 3 shows that the morphologies after the water has spread are dependent on the etching distance. There are two kinds of areas in the same film. One is the controlled assembling region in which the etching vacancy is the center; the other is the freely assembling region, which is determined by the density of the carbon nanotube film. The freely assembling region is decreased as the etching vacancy distance decreases (the etching distance is 150 μm and 100 μm in Figures 3a and 3b, respectively). When the etching distance approaches ≈ 40 μm, highly ordered aligned micropatterns are obtained without the freely assembling region because of the interference of the etching vacancies (Figure 3c), suggesting that if vacancies are arranged artificially, then various desired highly ordered polygon micropatterns may be fabricated.

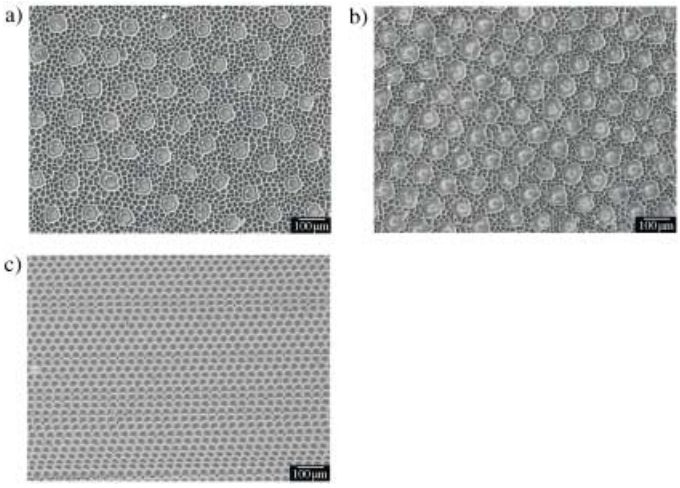

Figure 3. SEM images of micropatterned carbon nanotubes induced by water spreading on the laser-etched films with different etching distances: a) 150, b) 100, and c) 30 μm.

According to the above idea, ordered micropatterns were designed and obtained successfully by designing the position of the etching vacancies. The "wall" of the polygon is supposed to stand up approximately at the vertical bisector of two adjacent vacancies. Some designs of the etching positions are given in the inserts of Figure 4a–d, in which the

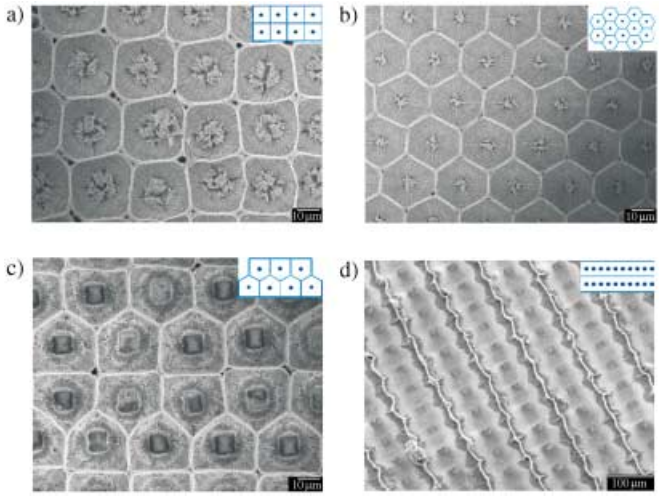

Figure 4. Highly ordered aligned patterns (a) cubic, b) hexagon, c) pentagon and d) parallel lines) are prepared by adjusting the arrangement of the vacancies. The inserts are the designs, the blue dots represent the laser etched vacancies and the blue lines the "walls" of carbon nanotubes.

blue dots represent vacancies and the lines represent "walls". In terms of these designs, the cubic, pentagonal, and hexagonal aligned micropatterns were fabricated (Figure 4a–c) by water spreading on the etched carbon nanotube film, and parallel lines were also formed in Figure 4d. All these demonstrate that large-scale aligned micropatterned structures can be obtained in a controlled fashion by water spreading and capillary force.

In summary, the present results provide evidence for self-assembly of carbon nanotubes to form large-scale 3D micropatterns through the water-spreading effect, and highly ordered patterned structures can be built controllably by adjusting the density of carbon nanotubes films artificially. Two-dimensional carbon nanotube films can be easily transformed into three-dimensional architectures after the growth of the film. This method might not only be extended to both inorganic nanotube/wire arrays[26,27] and organic nanotubes/fibers[28–30] to realize the transformation of 1D and 2D to 3D architectures, but also useful in fabricating microelectrical devices as well.

Experimental Section

Aligned carbon nanotubes films were prepared on cleaned quartz glass plates by pyrolysis of iron(II) phthalocyanine (FePc), which contains both the carbon source and the iron catalyst required. FePc (0.23 g) in a quartz boat was decomposed at approximately 550 °C, and the carbon nanotube film was prepared at approximately 900 °C in a flow reactor consisting of a quartz tube and a tube furnace fitted with a temperature controller under Ar/H_2. The growth time of the carbon nanotube films in this case was 5 min. After that, a water drop was carefully placed on the films. The artificial vacancies were induced by the Pulse Laser Etching System with 355 nm (New Wave Research Inc. in California), the size of the facula was 35×35 (2–3 μm) and the energy was 1.8–2.9 μW.

Optical microscope images were obtained on Olympus TH3 optical microscopy equipped with a CCD camera. SEM images were obtained on a JEOL JSM-6700F scanning electron microscope at 3.0 kV. Transmission electron microscopy images were obtained with an Hitachi JEM 200-CX instrument at 120 kV.

Received: May 27, 2003
Revised: November 17, 2003 [Z51988]

Keywords: carbon · electron microscopy · nanotubes · self-assembly · water

[1] T. Nishikawa, J. Nishida, R. Ookura, S. Nishimura, S. Wada, T. Karino, M. Shimomura, *Mater. Sci. Eng. C* **1999**, *10*, 141 – 146.
[2] H. Shimoda, S. J. Oh, H. Z. Geng, R. J. Walker, X. B. Zhang, L. E. McNeil, O. Zhou, *Adv. Mater.* **2002**, *14*, 899 – 901.
[3] N. Bowden, A. Terfort, J. Carbeck, G. M. Whitesides, *Science* **1997**, *276*, 233 – 235.
[4] Z. F. Ren, Z. P. Huang, J. W. Xu, J. H. Wang, P. Bush, M. P. Siegal, P. N. Provencio, *Science* **1998**, *282*, 1105 – 1107.
[5] L. Dai, A. W. H. Mau, *Adv. Mater.* **2001**, *13*, 899 – 913.
[6] S. Fan, M. G. Chapline, N. R. Franklin, T. W. Tombler, A. M. Cassell, H. Dai, *Science* **1999**, *283*, 512 – 514.
[7] S. Sun, C. B. Murray, D. Weller, L. Folks, A. Moser, *Science* **2000**, *287*, 1989 – 1992.
[8] S. Huang, A. W. H. Mau, T. W. Turney, P. A. White, L. Dai, *J. Phys. Chem. B* **2000**, *104*, 2193 – 2196.
[9] Y. Yang, S. Huang, H. He, A. W. H. Mau, L. Dai, *J. Am. Chem. Soc.* **1999**, *121*, 10832 – 10833.
[10] X. Wang, Y. Liu, D. Zhu, *Appl. Phys. A* **2000**, *71*, 347 – 348.
[11] H. Li, X. Wang, Y. Song, Y. Liu, Q. Li, L. Jiang, D. Zhu, *Angew. Chem.* **2001**, *113*, 1793 – 1796; *Angew. Chem. Int. Ed.* **2001**, *40*, 1743 – 1746.
[12] S. Li, H. Li, X. Wang, Y. Song, Y. Liu, L. Jiang, D. Zhu, *J. Phys. Chem. B* **2002**, *106*, 9274 – 9276.
[13] S. H. Park, D. Qin, Y. Xia, *Adv. Mater.* **1998**, *10*, 1028 – 1032.
[14] Y. Xia, J. A. Rogers, K. E. Paul, G. M. Whitesides, *Chem. Rev.* **1999**, *99*, 1823 – 1848.
[15] A. Ulman, *Chem. Rev.* **1996**, *96*, 1533 – 1554.
[16] S. A. Jenekhe, X. L. Chen, *Science* **1999**, *283*, 372 – 375.
[17] N. Maruyama, T. Koito, J. Nishida, T. Sawadaishi, X. Cieren, K. Ijiro, O. Karthaus, M. Shimomura, *Thin Solid Films* **1998**, *327–329*, 854 – 856.
[18] B. Q. Wei, R. Vajtai, Y. Jung, J. Ward, R. Zhang, G. Ramanath, P. M. Ajayam, *Nature* **2002**, *416*, 495 – 496.
[19] J. Jin, T. Iyoda, C. Cao, Y. Song, L. Jiang, T. Li, D. Zhu, *Angew. Chem.* **2001**, *113*, 2193 – 2196; *Angew. Chem. Int. Ed.* **2001**, *40*, 2135 – 2138.
[20] G. Decher, *Science* **1997**, *277*, 1232 – 1237.
[21] M. P. Pileni, *Langmuir* **1997**, *13*, 3266 – 3276.
[22] A. W. Adamson, A. P. Gast, *Physical Chemistry of Surfaces*, New York, Wiley, **1997**, pp. 358 – 359.
[23] E. W. Weisstein, *Handbook of Chemistry and Physics*, 61st ed., CRC Press, Boca Raton, FL, **1981**, p. F-45
[24] J. Z. Liu, Q. S. Zheng, Q. Jiang, *Phys. Rev. B.* **2003**, *67*, o75414-1–o75414-8.
[25] J. Z. Liu, Q. S. Zheng, Q. Jiang, *Phys. Rev. Lett.* **2001**, *86*, 4843 – 4846.
[26] J. Wu, S. Liu, *Adv. Mater.* **2002**, *14*, 215 – 218.
[27] Z. Zhang, G. Ramanath, P. M. Ajayan, D. Goldberg, Y. Bando, *Adv. Mater.* **2001**, *13*, 197 – 200.
[28] G. Shi, S. Jin, G. Xue, C. Li, *Science* **1995**, *267*, 994 – 996
[29] M. Fu, Y. Zhu, R. Tan, G. Shi, *Adv. Mater.* **2001**, *13*, 1874 – 1877.
[30] H. Qiu, M. Wan, B. Matthews, L. Dai, *Macromolecules* **2001**, *34*, 675 – 677.

